iScience

CellPress
OPEN ACCESS

Article

Pigmented skin exhibits accelerated wound healing compared to the nonpigmented skin in Guinea pig model

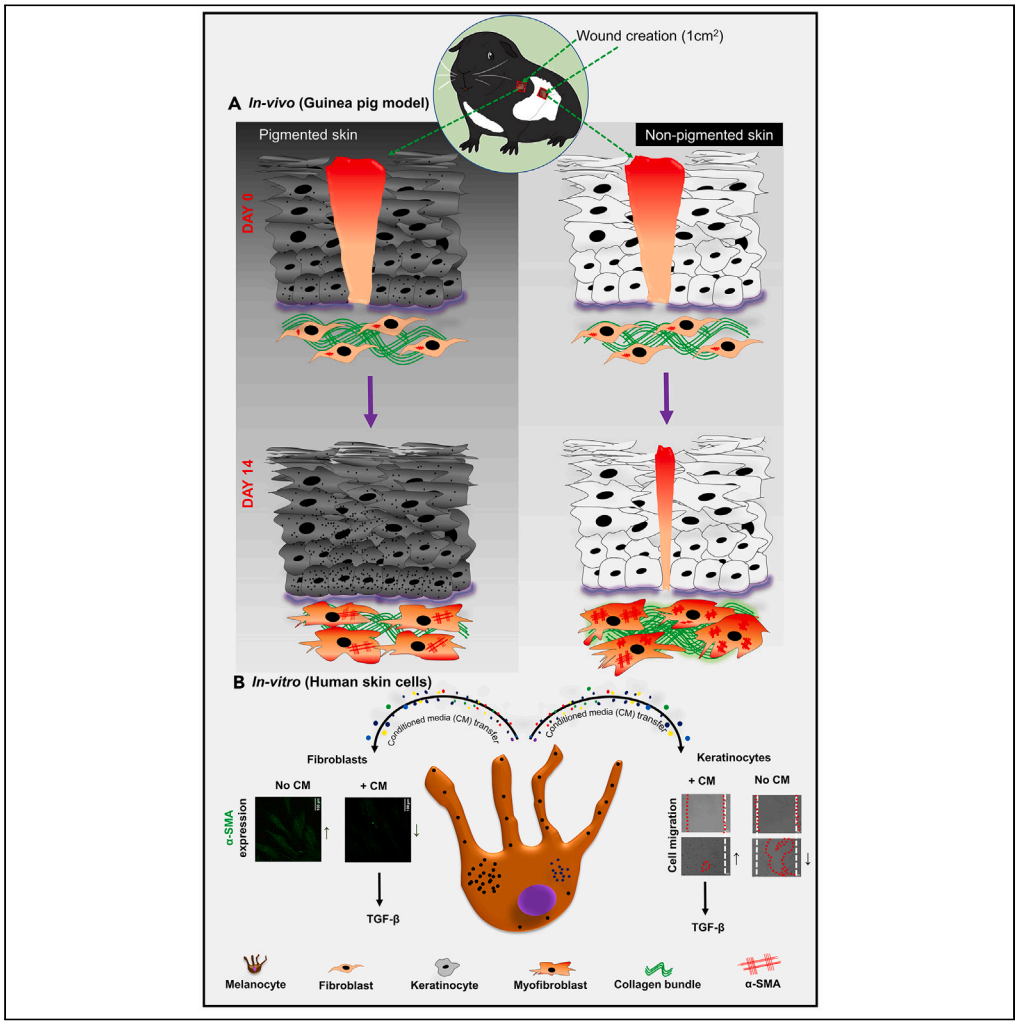

Rohit Gupta, Anshu Priya, Manish Chowdhary, ..., Perumal Nagarajan, Rajesh S. Gokhale, Archana Singh

rsg@nii.ac.in (R.S.G.)
archana@igib.res.in (A.S.)

Highlights

Pigmented (black) skin in guinea pigs contains melanin-rich cells in epidermis

Pigmented skin exhibits accelerated healing compared to non-pigmented skin

Melanin-rich cells begin to appear during proliferative phase in pigmented skin

Melanocyte conditioned media contains TGF- β, which promotes keratinocyte migration

Gupta et al., iScience 26, 108159
November 17, 2023
https://doi.org/10.1016/j.isci.2023.108159

iScience

CellPress
OPEN ACCESS

Article

Pigmented skin exhibits accelerated wound healing compared to the nonpigmented skin in Guinea pig model

Rohit Gupta,[1,2] Anshu Priya,[1,2,6] Manish Chowdhary,[1,2,6] Vineeta V. Batra,[3] Jyotsna,[4] Perumal Nagarajan,[4] Rajesh S. Gokhale,[4,5,*] and Archana Singh[1,2,7,*]

SUMMARY

This study investigated and compared the wound healing kinetics of pigmented (PG) and non-pigmented (NP) skin in guinea pigs, focusing on histological and transcriptional changes. Full-thickness wounds created on PG and NP skin were evaluated at various time points post-injury. Fontana-Masson staining and ultrastructural analysis suggested the presence of melanin and melanosomes in PG skin, which coincided with an upregulation of melanogenic genes cKIT, TYR, and DCT. On day 9 post-wound, PG skin exhibited a rapid transition from the inflammatory to proliferative phase, which correlated with the reappearance of epidermal pigmentation whereas the NP skin exhibited a delayed neo-epidermis formation. Furthermore, the study revealed that melanocyte-derived growth factors (conditioned media) positively regulated keratinocyte migration while inhibiting fibroblast differentiation. These effects were more prominent in tyrosine-treated (hyperpigmented) melanocyte-CM as was TGF- β expression. These findings provide valuable insights into the mechanisms underlying skin repair and pigmentation.

INTRODUCTION

A closely coordinated physical as well as molecular interaction between keratinocytes, melanocytes, and fibroblasts is essential for restoring the integrity of skin after physiological insults like wounds.[1] Although the roles of the individual components of wound repair have been largely delineated, the contribution of melanocytes in the healing process remains elusive.

Melanocytes are dendritic, neural crest-derived cells that produce melanin, protecting the skin from ultraviolet radiation and stress caused by generation of reactive oxygen species.[2] The role of melanocytes in wound healing was observed as early as the 1950s when they were found to be present in the newly formed epithelial covering within 4–6 days following wounding.[3] It is now known that following injury, melanocyte stem cells (McSCs) leave their niche within the bulge of the hair follicles and migrate to the injured epidermis, giving rise to differentiated melanocytes and resulting in the repigmentation of the epidermis.[4] The fact that these stem cells move out of their protected niche even before their initial cell division, only to repigment the wounded epidermis, is quite surprising and points toward their role in other important functions, like regulating keratinocyte differentiation.[4,5]

A recent study from our group had revealed a significant delay in the proliferative phase of wound healing in melanocyte-deprived skin of patients with vitiligo as compared to their corresponding non-lesional skin.[6] However, evaluation of healing efficiency during other phases of wound healing could not be undertaken due to constraints in taking human samples at multiple time points. Thus, we decided to study wound healing in a guinea pig model which, like human skin, harbors melanocytes within the interfollicular epidermis (IFE) and hair follicles. In the present study, we compared the wound healing efficiency of melanocyte-rich (pigmented) and melanocyte-deprived (non-pigmented) skin at histological and molecular (transcriptional) levels during the three phases of wound healing (inflammatory phase, re-epithelialization, and re-modeling) and found a significantly accelerated transition from inflammatory to re-epithelialization phase in the pigmented skin of guinea pigs.

[1]CSIR-Institute of Genomics and Integrative Biology, New Delhi 110025, India
[2]Academy of Scientific and Innovative Research, Ghaziabad 201002, India
[3]Govind Ballabh Pant Hospital, New Delhi 110002, India
[4]National Institute of Immunology, New Delhi 110067, India
[5]Present address: Indian Institute of Science Education and Research, Pune, Maharashtra, India
[6]These authors contributed equally
[7]Lead contact
*Correspondence: rsg@nii.ac.in (R.S.G.), archana@igib.res.in (A.S.)
https://doi.org/10.1016/j.isci.2023.108159

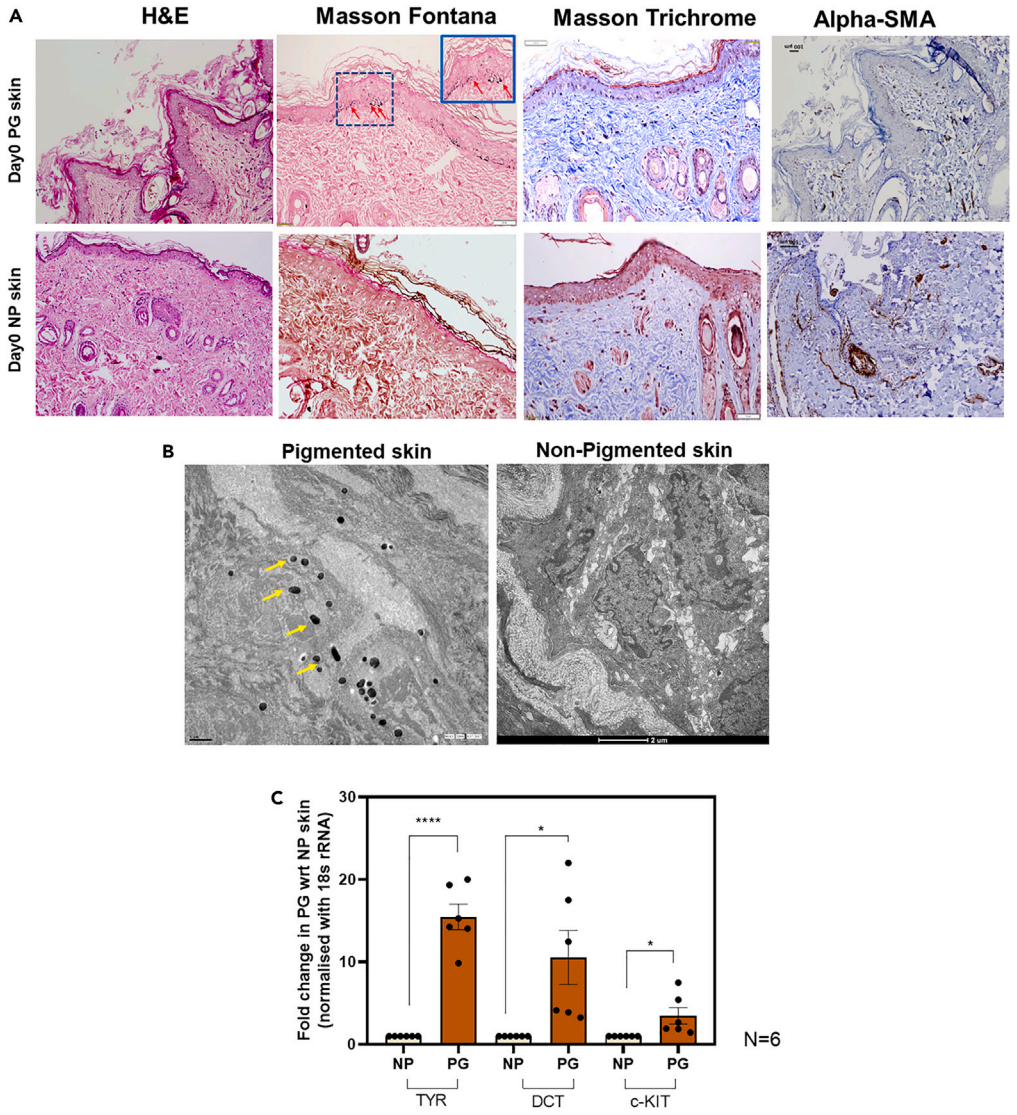

Figure 1. Histological evaluation of pigmented and non-pigmented skin in guinea pig (day0)

(A) Representative images of pigmented and non-pigmented skin sections (day 0 i.e., baseline) in guinea pigs using hematoxylin and eosin (H&E), Fontana-Masson (melanin, red arrows indicating melanin-positive cells), Masson Trichrome (collagen), and α-SMA (immunohistochemical staining) staining. Scale bar is 100 microns.

(B) Representative photomicrographs of TEM sections of pigmented and non-pigmented skin. Basal keratinocytes in pigmented skin showing electron-dense melanosomes (yellow arrows) while no melanosomes are observed in non-pigmented basal keratinocytes.

(C) Bar graph showing expression of three genes (fold change) involved in melanogenesis: tyrosinase (TYR), dopachrome tautomerase (DCT), and cKIT (n = 6). 18srRNA was used for internal normalization. $p < 0.05$ was considered statistically significant. Error bar represents standard error of mean. PG: pigmented skin; NP: non-pigmented skin.

See also Figure S2.

RESULTS

Histological, ultrastructural, and molecular evaluation of pigmented and non-pigmented skin in guinea pigs: basal state (day 0)

Hematoxylin & Eosin (H&E) staining of skin sections (day0) revealed 2–3 layers-thick stratified epidermis in both pigmented (PG) and non-pigmented (NP) skin (Figure 1A). In the dermis region, several hair follicles were observed in comparable numbers in both the NP and PG skin (Figure S2).

As antibody reactive against guinea pig S100 (marker for melanocytes) was not available commercially, we performed Fontana-Masson staining to detect melanin (as a proxy for melanocytes and/or melanocyte-mediated melanin transferred to the keratinocytes), which revealed presence of melanin-rich cells only in the epidermis of PG skin (Figure 1A). Transmission electron microscopy of NP and PG skin samples

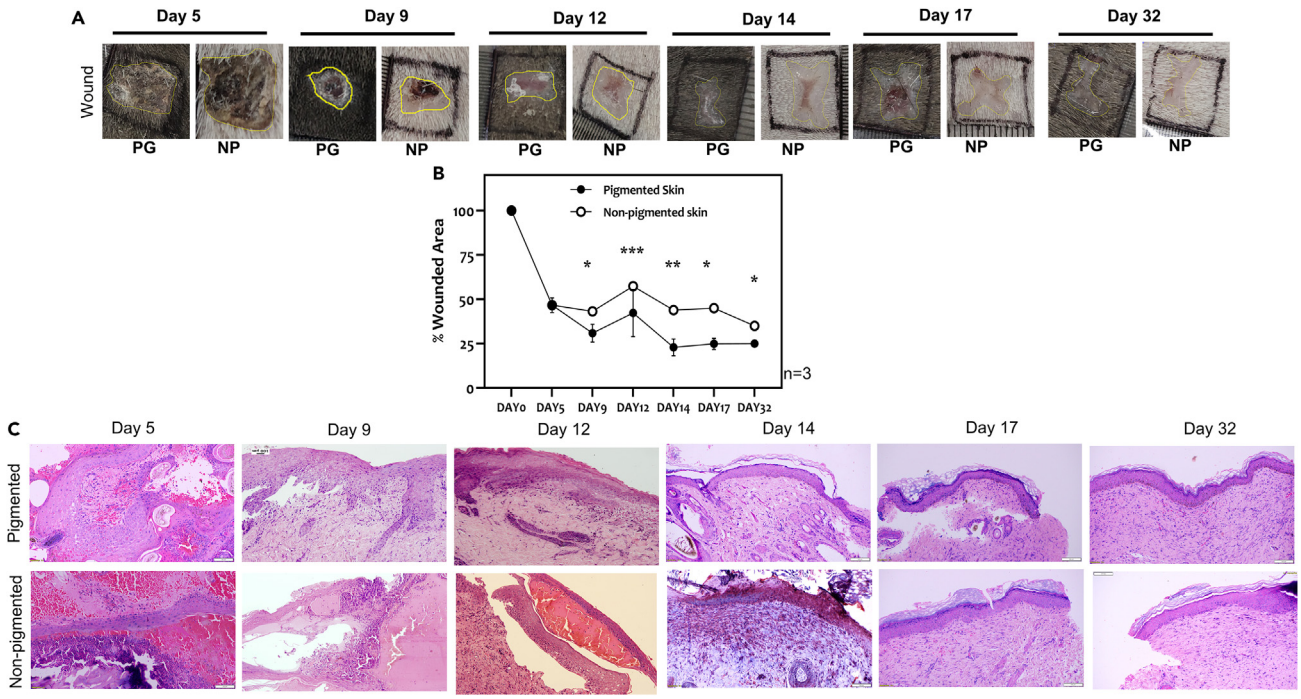

Figure 2. Morphometric and histological evaluation of pigmented and non-pigmented guinea pig skin during wound healing

(A) Representative images at day 5, day 9, day 12, day 14, day 17, and day 32 post-wound in pigmented and non-pigmented skin. Black square represents initial wound size of 1 cm × 1 cm.

(B) Line graph depicting percentage wounded area remaining at day 5, day 9, day 12, day 14, day 17, and day 32 post-wound in pigmented and non-pigmented skin based on morphometric evaluation of wounds (n = 3). p value < 0.05 was considered statistically significant. Error bar represents standard error of mean.

(C) Representative images of H&E-stained skin sections (10x magnification) of pigmented and non-pigmented skin at day 5, day 9, day 12, day 14, day 17, and day 32 post-wound in guinea pigs. Scale bar represents 100 microns.

See also Figure S3.

revealed the presence of melanosomes only in the PG skin (Figure 1B). Further, we evaluated the transcript levels of key genes expressed in melanocytes (TYR, DCT, cKIT) and found a significant increase in their expression levels in PG compared to NP skin (Figure 1C), consistent with the ultrastructural and histological findings.

The collagen organization as revealed by Masson trichrome and α-SMA staining (which stains alpha-smooth muscle actin expressed by myofibroblasts as well as blood vessels) was comparable between NP and PG skin (Figure 1A). Taken together, PG and NP skin appeared to be similar at the histological and ultrastructural level, except for the presence of melanin/melanosomes in the former.

Morphometric and histological evaluation of wound healing reveals accelerated wound closure in pigmented compared to non-pigmented skin

Morphometric analysis of wounds revealed comparable healing on day 5 in both pigmented and non-pigmented skin, however, a significantly higher wound closure was observed on day 9 in the pigmented skin ($p < 0.05$, Figures 2A and 2B). By the 12th day, the wounded area had closed completely in both PG and NP skin, with formation of a visible scar in the center of the wound. However, PG skin presented with a significantly reduced scar tissue on day 12 ($p < 0.001$), day 14 ($p < 0.001$), day 17 ($p < 0.02$) as well as day 32 ($p < 0.04$) (Figures 2A and 2B) when compared to corresponding non-pigmented skin.

H&E staining of skin sections revealed focal ulceration, characteristic of the inflammatory phase of healing, predominantly consisting of polymorphonuclear cells (PMNs) in both PG and NP skin on the 5th day post-wound (Figure 2C). While this ulceration resolved considerably by day 9/day 12 in both PG and NP skin, a neo-epidermis, suggestive of initiation of re-epithelialization, was observed only in the pigmented skin (Figure 2C). By day 14, the NP skin also presented with a well-formed neo-epidermis along with a thin layer of stratum corneum along with the appearance of dermal infiltrates including fibroblasts as well as dermal appendages (Figures 2C and S3). Overall, the histological evaluation revealed an accelerated re-epithelialization in PG as compared to NP skin, especially in the initial phases of healing. Based on the histological evaluation, day 5 and day 9 coincided with the inflammatory phase; days 12, 14, and 17 represented the re-epithelialization phase and day 32 corresponded to the remodeling phase of wound healing.

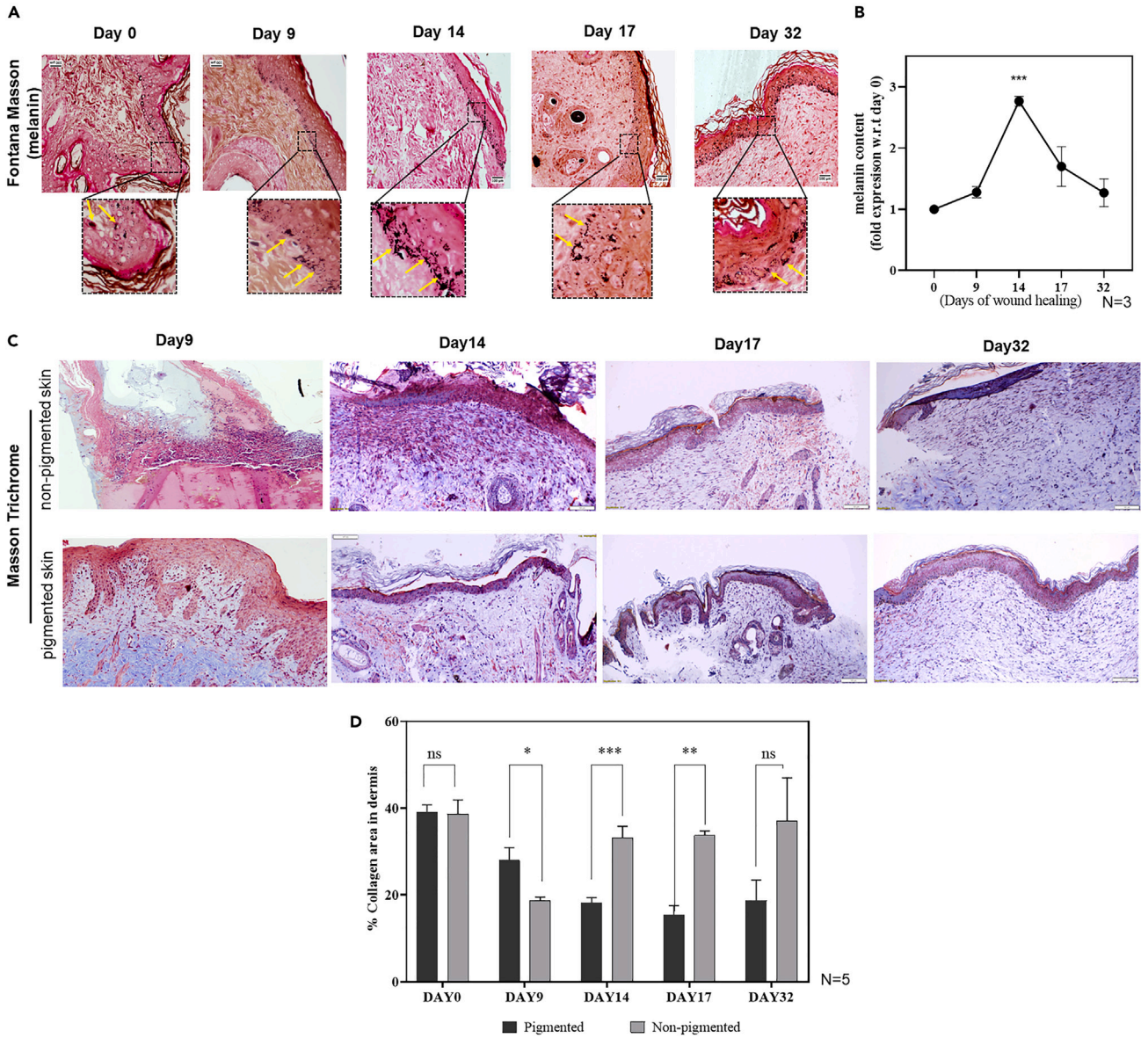

Figure 3. Melanin content and collagen deposition in pigmented and non-pigmented skin during wound healing

(A) Representative images of sections stained with Fontana-Masson (melanin) in the pigmented skin at day 0 (baseline), day 9, day 14, day 17, and day 32 post-wound in guinea pigs.

(B) Graph depicting quantification of melanin content present in entire epidermis in the pigmented skin (n = 3).

(C) Representative images of Masson Trichrome (collagen) stained pigmented and non-pigmented skin at day 9, day 14, day 17, and day 32 post-wound and (D) its quantitation using ImageJ analysis (n = 5). Error bar represents standard error of mean. p value <0.05 was considered statistically significant.

See also Figure S4.

Melanin content and collagen deposition are differentially regulated in pigmented and non-pigmented skin during wound healing

Melanin estimation of Fontana Masson-stained sections suggested that the pigmentation began to appear as early as day 9 in the epidermis of pigmented skin and peaked during the proliferative phase (day 14), where it increased to almost 2-fold compared to day 0, after which it steadily declined (day 17) and reached to almost basal levels by day 32. (Figures 3A and 3B). The collagen deposition (Masson Trichrome staining), which was found to be lower in non-pigmented skin on day 9 perhaps owing to poor re-epithelialization, showed significantly increased collagen deposition during late proliferative phase of healing (day 14, day 17), suggestive of increased extracellular matrix (ECM) formation in NP compared to pigmented skin (Figures 3C and 3D). Immunohistochemistry for α-SMA revealed presence of a

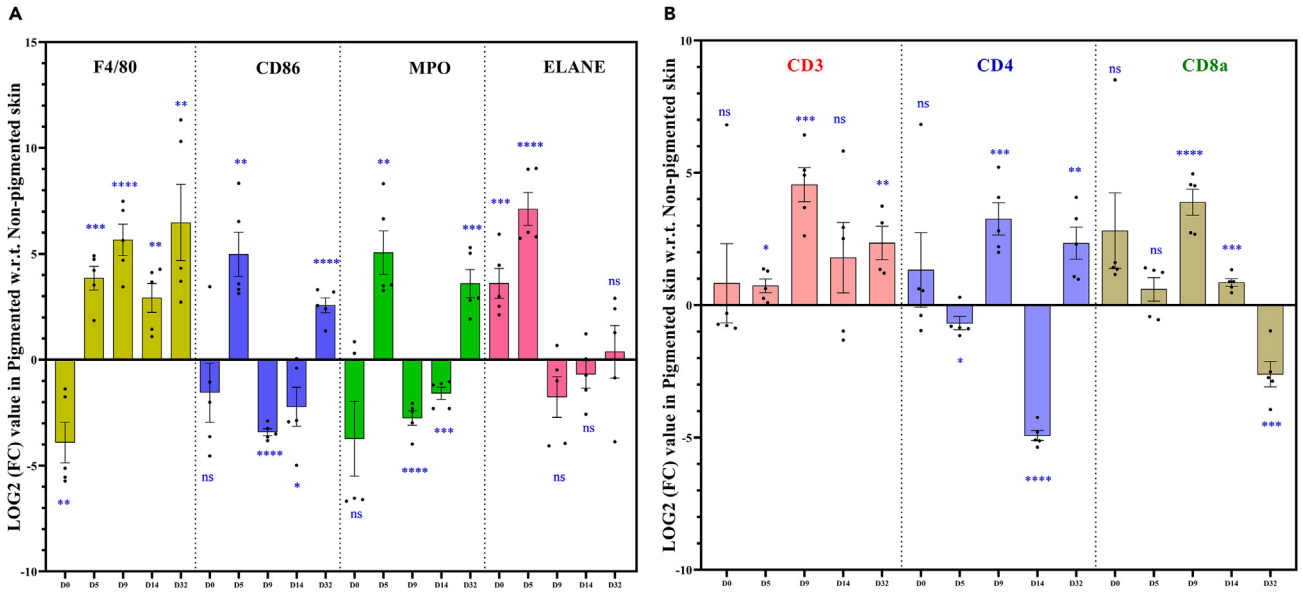

Figure 4. Markers of macrophages, neutrophils, and T cells are differentially regulated in pigmented skin during wound healing

(A) Scatterplot with bar graph where bar represents log2FC values ±standard error of mean (SEM) for transcripts of ELANE and MPO, markers of neutrophils and of macrophage markers, CD86 and F4/80. Each point on the bar represented log2FC for individual samples (n = 5).

(B) Scatterplot with bar graph where bar represents average log2FC values ±standard error of mean (SEM) for transcripts of CD3, CD4, and CD8a. Each point on the bar represents log2FC for individual samples (n = 5). p value <0.05 was considered statistically significant.

See also Figures S5–S7.

significantly higher number of α-SMA-positive dermal fibroblasts in the NP compared to PG skin, consistent with the pattern observed for collagen content (Figure S4).

Pigmented skin exhibits differential infiltration of macrophages, neutrophils, and T cells compared to non-pigmented skin during wound healing

Based on the histological evaluation of skin tissue, we selected 4 time points: day 5 (inflammatory phase), day 9, day 14 (proliferative phase), and day 32 (remodeling phase) for studying the changes at the molecular level. Expression of immune cell markers and dermal-epidermal cell markers in the pigmented skin was compared to the corresponding time points in the non-pigmented skin.

The infiltration of neutrophils, one of the most dominant cell types found in the inflammatory phase, was evaluated by analyzing expression of two markers- myeloperoxidase (MPO) and elastase (ELANE). Both the markers showed significant upregulation on day 5, after which their expression declined significantly when compared to the non-pigmented skin (Figures 4A and S5). The expression of macrophage markers (F4/80 and CD86) was also significantly upregulated on day 5 in the pigmented compared to non-pigmented skin (Figures 4A and S5). These results suggested an increased infiltration of neutrophils and macrophages in PG compared to NP skin during inflammatory phase of healing.

Pigmented skin exhibits differential expression of inflammatory and anti-inflammatory cytokines compared to the non-pigmented skin during wound healing

In addition to the neutrophils and macrophages, $CD4^+$ T cells and $CD8^+$ T cells also play a crucial role in regulating the kinetics of wound healing. We therefore checked expression (transcript level) of CD3 (pan T cell marker), CD4, and CD8alpha using RT-PCR. Expression of all the three markers was significantly increased in the PG skin on day 9 (Figures 4B and S6), which marked the transition from inflammatory to the proliferative phase. Immunohistochemistry for guinea pig-specific $CD4^+$ T cells showed presence of these cells in the dermis, however, it was difficult to quantitate the signals due to presence of non-specific signals (Figure S7). Altered expression of immune cells in pigmented vs. non-pigmented skin prompted us to analyze the expression level of inflammatory (TNF-α, IL1-β, and CCL2) and anti-inflammatory cytokines (TGF-β and IL-10) during different phases of wound healing. All the cytokines, except IL-10, were significantly upregulated in the inflammatory phase (day 5) (Figures 5A, S8A, and S8B). However, in the proliferative phase, that is, day 9 and day 14, the inflammatory cytokines were significantly downregulated, whereas the anti-inflammatory cytokines showed a significant upregulation in the pigmented skin when compared to the non-pigmented skin (Figures 5A, S8A, and S8B). Analysis of IFN-γ and IL-2, other important cytokines produced by immune cells, also showed a consistent upregulation of IL-2 from day 5 to day 14 whereas IFN-γ was found to be upregulated only on day 5, after which its expression was downregulated compared to non-pigmented skin (Figures 5A and S8B). As cell proliferation and angiogenesis are important aspects of wound healing, we checked the gene expression of two proliferation markers, Ki67 and MCM6

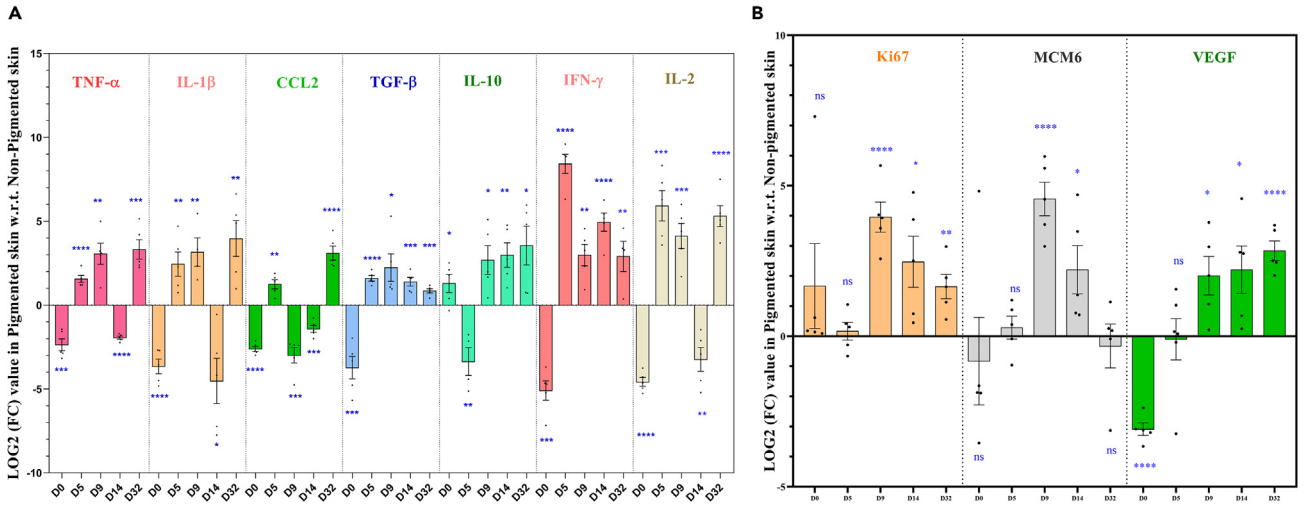

Figure 5. Differential expression of inflammatory and anti-inflammatory cytokine in pigmented compared to non-pigmented skin

(A) Scatterplot with bar graph where bar represents average log2FC values ±standard error of mean (SEM) for transcripts of inflammatory (CCL2, IL1-β, and TNF-α) and anti-inflammatory cytokines (IL-10 and TGF-β) and IL-2 and IFN-γ. Each point on the bar represented log2FC for individual samples (n = 5).

(B) Scatterplot with bar graph where bar represents average log2FC values ±standard error of mean (SEM) for transcripts of proliferation markers Ki67, MCM6 and angiogenesis marker VEGF. Each point on the bar represents log2FC for individual samples (n = 5). p value <0.05 was considered statistically significant. See also Figures S8A, S8B, and S9.

(minichromosome maintenance 6) and VEGF, a marker for angiogenesis during different days of wound healing. Expression of Ki67 and VEGF was significantly increased in pigmented skin during proliferative and remodeling phases (D9, D14, and D32) while expression of MCM6 was increased at day 9 and day 14 in the PG skin compared to NP skin (Figures 5B and S9).

Melanocyte-derived growth factors promote keratinocyte migration

The higher melanin content in the re-epithelialized neo-epidermis in the pigmented skin compared to its basal level (day 0), as revealed in the histological studies, was intriguing and prompted us to investigate if melanocytes and/or melanin content could regulate physiology of keratinocytes during wound healing.

In order to investigate whether melanocytes could differentially regulate wound re-epithelialization, we designed *in vitro* experiments to assess keratinocyte migration where we added conditioned media derived from primary melanocyte cultures to HaCaT keratinocytes and performed scratch wound assay. Conditioned media was collected from melanocytes treated with three different conditions:vehicle treated (basal level pigmentation, that is, control melanocytes), tyrosine-treated melanocytes (relatively hyperpigmented compared to control), and third condition where the number of melanocytes was doubled (2X to simulate proliferation) but treated with phenylthiourea or PTU, a known chemical that inhibits melanin synthesis in melanocytes (hypopigmented 2X MC). Compared to untreated keratinocytes, cells treated with conditioned media from melanocytes (vehicle control) showed significantly higher migration. Conditioned media from hyperpigmented melanocytes promoted the migration of keratinocytes to the greatest extent. A significant migration was also observed when keratinocytes were treated with conditioned media from hypopigmented 2X melanocytes. However, the mere addition of melanin (synthetic) in keratinocytes did not promote keratinocyte migration (Figures 6C and 6D). These results suggested that substances secreted by melanocytes and not the presence of melanin per se (exogenous) induced keratinocyte migration. However, melanocyte-conditioned media did not significantly alter the proliferation potential of keratinocytes as analyzed by cell cycle assay (Figure S10). At molecular level, melanocyte-conditioned media had no effect on the expression levels of keratin 14 transcript (proliferation marker), however, it significantly enhanced expression of keratinocyte differentiation marker, involucrin (Figure S11), suggesting that melanocyte-derived factors could promote keratinocyte differentiation.

Melanocyte-derived growth factors modulate fibroblast differentiation and proliferation

In addition to keratinocytes, fibroblasts too play an important role in modulating the kinetics of wound re-epithelialization. A significantly lower collagen deposition during proliferative phase (day 14 and 17) which coincided with a higher melanin content in the pigmented skin prompted us to investigate if melanocytes and/or melanin could influence fibroblast biology, especially their proliferation potential and the ability to differentiate into myofibroblasts. We therefore treated primary fibroblast cultures with conditioned media from melanocytes (basal pigment level or tyrosine-treated) or with synthetic melanin and measured expression of Ki67, a proliferation marker, using ICC. Fibroblasts treated with TGF-β served as a control. Compared to no conditioned media control, keratinocytes treated with conditioned media from melanocytes (both basal pigmentation and tyrosine-treated) showed significantly higher Ki67 positivity, while addition of exogenous melanin did not promote proliferation (Figures 6E and 6F). For the differentiation analysis, TGF-β treatment expectedly resulted in a significant

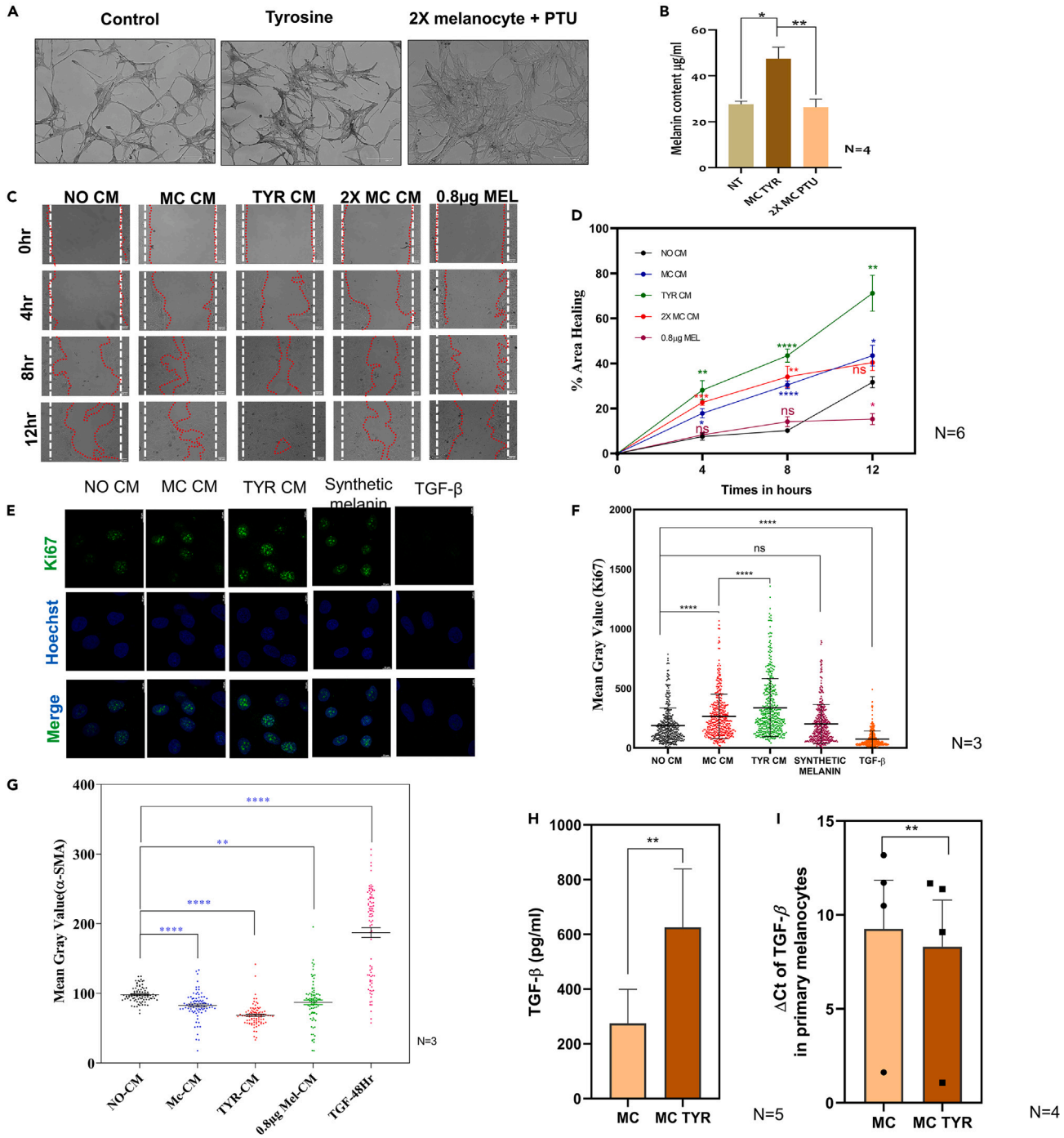

Figure 6. Melanocyte-derived growth factors regulate keratinocytes and fibroblasts during wound healing

(A) Representative microscopic images and (B) melanin quantification of primary human melanocytes treated with vehicle control, 100µM L-tyrosine or 2X melanocytes treated with 100µM phenylthiourea (2Xmelanocytes+PTU).

(C) Scratch wound assay depicting the migration of keratinocytes (HaCaT) treated with 25% conditioned media (CM) from tyrosine-treated (TYR CM), 2XMelanocytes+PTU (2X MC CM), control melanocytes with basal level of pigmentation (MC CM), 0.8µg synthetic melanin or no conditioned media (No CM). White dotted lines depict wound area at t = 0 h (starting point), and red dotted line depicts the area migrated by keratinocytes at different time points.

(D) Quantification of percentage healing (of scratch wound) at 0, 4, 8 and 12 h (N = 6). Error bar represents standard error of mean. Keratinocyte migration upon different treatments was compared with migration observed in keratinocytes treated with "no conditioned media" (No CM) and p values are depicted in corresponding colors.

Figure 6. *Continued*

(E) Immunocytochemical staining for Ki67 (green) in fibroblasts treated with melanocyte conditioned media: no conditioned media (No CM), control melanocytes with basal level of pigmentation (MC CM), tyrosine treated hyperpigmented melanocytes (TYR CM), synthetic melanin or TGF-β (5 ng/ml, positive control). Hoechst dye was used as a nuclear counterstain and (F) quantitation of Ki67 positivity (n = 3 experiments).

(G) Quantitation of alpha-SMA positivity (ICC images) in fibroblasts treated with melanocyte conditioned media. No conditioned media (No CM), control melanocytes with basal level of pigmentation (MC CM), tyrosine treated hyperpigmented melanocytes (TYR CM), synthetic melanin (Mel-CM) and TGF-β (5 ng/ml, positive control). p values less than 0.05 was considered statistically significant. Error bar represents standard error of mean.

(H) TGF-β levels in melanocyte cultures as detected by ELISA assay (n=5).

(I) Scatter plot with bar graph showing ΔCt values of transcript of TGF-β in melanocyte cultures (n=4). MC: melanocytes with basal pigmentation; MC TYR: tyrosine-treated melanocyte supernatants. p value <0.05 was considered statistically significant.

See also Figures S10–S15.

induction of α-SMA, whereas melanocyte conditioned media (basal pigmentation as well as tyr-treated) resulted in a significant decrease in α-SMA positive cells (Figures 6G and S12). RT-PCR analysis also revealed a significant downregulation of α-SMA and Col1A (collagen 1A) expression upon treatment with melanocyte-conditioned media as depicted in Figure S13.

Melanocyte-derived TGF-β regulates migration potential of keratinocytes

In an attempt to underpin the factors/pathways present in melanocyte-conditioned media that could potentially regulate keratinocyte migration, we focused our efforts on the role of TGF- β as it has previously been shown to be not only produced by melanocytes [26] but has also been shown to promote keratinocyte migration [27]. We, therefore, measured the levels of TGF β (ELISA assay) in the melanocyte supernatants and found increased TGF-β in melanocytes treated with tyrosine (mean 72 pg/ml) compared to control melanocytes containing basal level pigmentation (mean 199 pg/ml) (Figure 6H). Additionally, we also investigated transcript levels of TGF-β in tyrosine-treated melanocytes and control melanocytes (basal level pigmentation) and found significantly increased TGF-β in tyrosine-treated cells (more than 2-fold change compared to control, Figures 6I and S14). As a positive control, we checked the effect of the exogenous addition of TGF-β (1 ng/ml and 5 ng/ml) on keratinocyte migration using scratch wound assay and found accelerated keratinocyte migration compared to vehicle control, confirming that TGF-β could indeed promote keratinocyte migration (Figure S15). Taken together, these results suggest that melanocyte-derived TGF-β promoted keratinocyte migration.

DISCUSSION

Paracrine signaling among melanocytes-keratinocytes-fibroblasts is key to maintain normal skin homeostasis. In events of physiological stress, like skin injury, a complex spatiotemporal interplay among keratinocytes, fibroblasts, and transiently recruited immune cells ensues and restores skin integrity. However, the role of melanocytes in this repair process is largely undefined due to our current understanding of the kinetics of wound healing process being derived from the skin of mice[7] and rats,[8] both of which lack epidermal melanocytes (except in ear lobes and tail).

To overcome this caveat, we utilized guinea pig as a model organism, which harbors epidermal as well as follicular melanocytes like human skin and compared the wound healing kinetics in melanocyte-rich (pigmented) vs. melanocyte-deprived (non-pigmented) skin. Interestingly, the presence of a neoepidermis as early as the 9th day post-wound in pigmented skin compared to its appearance on 12th day in the non-pigmented skin was intriguing, and we, therefore, performed quantitative PCR-based expression analysis of various cell markers to unravel the molecular mechanisms underlying this remarkable difference in the kinetics of re-epithelialization.

The differential regulation of several cytokines on day 0 in PG compared to NP skin was intriguing. Downregulation of cytokines such as IFN-γ, TNF-α, and IL-2 in PG skin, which are known to modulate immune responses by inducing the development of functionally heterogeneous T cell populations,[9,10] suggested a difference in immune cell population as well as in immunological responses between the pigmented and non-pigmented skin. Interestingly, non-toxic concentrations of synthetic melanin have been previously demonstrated to suppress the production of cytokines such as TNF-α, IL-1β, and IL-10 by reducing the efficiency of mRNA translation.[11] Thus, it is tempting to infer that the downregulation of these cytokines could be due to the presence of melanin in PG skin.

During wound healing, immune cells of both innate and adaptive system are known to play an important role in fine-tuning its kinetics, especially the transition from inflammatory to proliferative phase. Macrophages, the innate immune cells, by effectively removing the neutrophils, are known to help in timely resolution of inflammation, enabling progression into the proliferative phase.[12,13] The importance of efficient removal of neutrophils by macrophages is further demonstrated in the cases of chronic diabetic wounds, wherein impaired removal of neutrophils by macrophages prolongs the inflammatory phase and delays healing.[14,15] Likewise, Treg, cells of adaptive system, are also known to impact wound healing, wherein its depletion causes impaired wound healing by suppressing excessive accumulation of T cells, altering the cytokine milieu of the wound.[16] Thus, a significant upregulation of macrophage marker F4/80, concomitant with a significant downregulation of neutrophils (ELANE and MPO) during the proliferative phase, together with upregulation of Treg in the inflammatory phase probably induced an accelerated transition to proliferative phase in the pigmented skin.

Recent studies suggest that in addition to the immune cells, melanocytes, via cross-talk with immune cells, can also influence the kinetics or the outcome of wound repair. For instance, melanocytes are known to communicate with macrophages in response to UV radiation,[17] besides being able to "control" immune responses by acting as potent inhibitors of T cell proliferation.[18,19] Interestingly, the presence of

macrophages and neutrophils and the ensuing inflammatory response is one of the cues known to promote melanocyte homing during early phase of wound healing.[20] Thus, a significant upregulation of macrophage and neutrophil markers during inflammatory phase in the pigmented skin could be a likely trigger for inducing melanocyte migration into the wound site, which then accelerates transition to the proliferative phase.

A higher than basal pigmentation observed during wound healing (proliferative phase) was consistent with previous reports,[3] however, its significance during the healing process is not fully known, partly due to use of animal models that lack inter-follicular melanocytes.[7,8] An accelerated migration of keratinocytes observed upon scratch wound assay performed in the presence of secretome from melanocytes with pointed to an important contribution of melanocyte-derived factors in skin homeostasis, beyond its canonical role of imparting color to the skin, warranting further investigations to offer more insights into this phenomenon.

As for the potential sources of melanocytes, the surrounding unwounded skin and the adnexal elements such as hair follicles could provide a rich source of melanocytes for repopulation into the scars,[4,21] depending on the depth of the wounds.[3] Coinciding with the appearance of dermal appendages from day 14 onwards in our study, hair follicle-derived melanocytes/McSCs seem to be the most probable source of the incoming melanocytes 14 days post-wound, while surrounding unwounded skin most likely contributed to the melanocytes during earlier time points (day 9 and day 12).

Another important difference observed during morphometric evaluation of pigmented and non-pigmented wounds was a higher scar formation in non-pigmented skin. Increased presence of myofibroblasts in the non-pigmented skin, probably resulting from a relatively higher expression of inflammatory cytokines IL1-β and CCL2 driving their differentiation into myofibroblasts.[22] Interestingly, a significantly reduced alpha-SMA expression upon treatment of fibroblasts with melanocyte-conditioned media suggested that melanocytes might regulate myofibroblast biology, likely explaining reduced scar formation in pigmented skin.

Contribution of melanocytes may become increasingly important in pathological conditions involving hyperpigmentation or hypopigmentation. For instance, in patients with vitiligo or albinism (with partially or completely depigmented skin, respectively), which comprise more than 2% of the world population, there is almost no incidence of hypertrophic scar or keloid formation (characterized by dense fibrous tissue post wound healing). In contrast, the incidence rate of keloids and hypertrophic scars in darkly pigmented individuals is abnormally high, underlining an important role of melanocytes in the process.[23] Therefore, knowing the molecular underpinnings of how melanocyte-derived cellular factors may regulate wound healing may offer crucial hints in developing new therapeutic modalities to enhance wound healing. Our *in vitro* experiments using human skin-derived fibroblasts, melanocytes, and keratinocytes suggested that secreted factors derived from melanocyte cultures could regulate keratinocyte migration and fibroblast differentiation potential, both of which are important aspects in determining efficiency of wound healing kinetics. Previous reports showing that TGF β is produced by melanocytes[24] and that TGF-β could modulate keratinocyte migration[25] prompted us to investigate if melanocytes modulated keratinocyte migration via secretion of TGF-β. Detection of significantly higher levels of TGF β in conditioned media of hyperpigmented compared to basal melanocytes was concomitant with the significantly higher migration observed in keratinocytes that were treated with conditioned media from hyperpigmented melanocytes. These studies suggested an important role of melanocytes in regulating keratinocyte and fibroblast biology, important determinants governing wound healing.

In summary, our study provides a comprehensive understanding of histological as well as molecular changes during wound healing in pigmented and non-pigmented skin of guinea pigs. Our study provides compelling evidence that pigmented skin exhibits accelerated transition from inflammatory to proliferative phase, which coincides with increased presence of melanin pigment in the newly formed epidermis layer.

Limitations of the study

The major limitation of the study is non-availability of molecular tools like antibodies against guinea pig antigens. However, since guinea pig skin is physiologically closer to that of humans (including the presence of interfollicular melanocytes), this model does provide important "initial step" toward understanding the mechanisms underlying differential wound healing kinetics in pigmented vs. non-pigmented skin. Moreover, the *in vitro* validation carried out in the present study using human skin-derived melanocytes, keratinocytes, and fibroblasts suggests an important role of melanocyte-derived growth factors in modulating wound healing kinetics by regulating keratinocytes and fibroblasts biology.

STAR★METHODS

Detailed methods are provided in the online version of this paper and include the following:

- KEY RESOURCES TABLE
- RESOURCE AVAILABILITY
  - Lead contact
  - Materials availability
  - Data and code availability
- EXPERIMENTAL MODEL AND STUDY PARTICIPANT DETAILS
  - Wound creation in guinea pigs
  - Ethics statement
- METHOD DETAILS

- Macroscopic evaluation of wounds
- Histology and special stains
- Quantitation of melanin and collagen content
- Transmission electron microscopy
- Total RNA extraction, cDNA synthesis and real time PCR
- RT-PCR data analysis
- Primary cultures of normal human epidermal melanocytes (NHEM) and normal human dermal fibroblasts (NHDF)
- Modulation of melanin content in melanocytes
- Melanin estimation in melanocytes
- Keratinocyte migration assay
- α-SMA and Ki67 staining in fibroblasts
- Immunohistochemistry (IHC) of α-SMA and CD4+T cells
- Cell cycle assay
- ELISA for TGF-β
- Statistical analysis

SUPPLEMENTAL INFORMATION

Supplemental information can be found online at https://doi.org/10.1016/j.isci.2023.108159.

ACKNOWLEDGMENTS

R.S.G. and A.S. acknowledge the support of Science and Engineering Research Board (SERB) project EMR/2016/007548 and A.S. acknowledges the support of MLP2008 project from Council of Scientific and Industrial Research (CSIR, India). The authors gratefully acknowledge the transmission electron microscopy (TEM) facility at CSIR-IGIB for the ultrastructural studies. R.S.G. acknowledges support from J.C. Bose fellowship.

AUTHOR CONTRIBUTIONS

Conceptualization, A.S. and R.S.G.; Methodology and investigation, R.G., A.P., M.C., and Jyotsna; Data Curation, R.G., A.P., and M.C.; P.N. facilitated housing of guinea pigs in the animal house and assisted in animal experiments. V.V.B. helped in conducting histological studies. Writing and funding acquisition, A.S. and R.S.G.; Supervision, A.S.

DECLARATION OF INTERESTS

R.S.G. is a co-founder of Vyome Biosciences Pvt. Ltd., a biopharmaceutical company working in the dermatology area.

Received: March 1, 2023
Revised: August 25, 2023
Accepted: October 5, 2023
Published: October 6, 2023

REFERENCES

1. Rodrigues, M., Kosaric, N., Bonham, C.A., and Gurtner, G.C. (2019). Wound Healing: A Cellular Perspective. Physiol. Rev. *99*, 665–706. https://doi.org/10.1152/physrev.00067.2017.
2. Janjetovic, Z., Jarrett, S.G., Lee, E.F., Duprey, C., Reiter, R.J., and Slominski, A.T. (2017). Melatonin and its metabolites protect human melanocytes against UVB-induced damage: Involvement of NRF2-mediated pathways. Sci. Rep. *7*, 1274. https://doi.org/10.1038/s41598-017-01305-2.
3. SNELL, R.S. (1963). A study of the melanocytes and melanin in a healing deep wound. J. Anat. *97*, 243–253.
4. Chou, W.C., Takeo, M., Rabbani, P., Hu, H., Lee, W., Chung, Y.R., Carucci, J., Overbeek, P., and Ito, M. (2013). Direct migration of follicular melanocyte stem cells to the epidermis after wounding or UVB irradiation is dependent on Mc1r signaling. Nat. Med. *19*, 924–929. https://doi.org/10.1038/nm.3194.
5. Paus, R. (2013). Migrating melanocyte stem cells: masters of disaster? Nat. Med. *19*, 818–819. https://doi.org/10.1038/nm.3264.
6. Gupta, A., Chauhan, A., Priya, A., Mantri, B., Wadhokar, M., Dalave, K., Shah, B., Gokhale, R.S., Batra, V.V., and Singh, A. (2020). Lesional skin in vitiligo exhibits delayed *in vivo* reepithelialization compared to the nonlesional skin. Wound Repair Regen. *28*, 307–314. https://doi.org/10.1111/wrr.12798.
7. Dunn, L., Prosser, H.C.G., Tan, J.T.M., Vanags, L.Z., Ng, M.K.C., and Bursill, C.A. (2013). Murine Model of Wound Healing. J. Vis. Exp. e50265. https://doi.org/10.3791/50265.
8. Dorsett-Martin, W.A. (2004). Rat models of skin wound healing: A review. Wound Repair Regen. *12*, 591–599. https://doi.org/10.1111/j.1067-1927.2004.12601.x.
9. Hossain, M.R., Ansary, T.M., Komine, M., and Ohtsuki, M. (2021). Diversified Stimuli-Induced Inflammatory Pathways Cause Skin Pigmentation. Int. J. Mol. Sci. *22*, 3970. https://doi.org/10.3390/ijms22083970.
10. O'Garra, A. (1998). Cytokines Induce the Development of Functionally Heterogeneous T Helper Cell Subsets. Immunity *8*, 275–283. https://doi.org/10.1016/S1074-7613(00)80533-6.
11. Mohagheghpour, N., Waleh, N., Garger, S.J., Dousman, L., Grill, L.K., and Tusé, D. (2000). Synthetic Melanin Suppresses Production of Proinflammatory Cytokines. Cell. Immunol. *199*, 25–36. https://doi.org/10.1006/cimm.1999.1599.
12. Meszaros, A.J., Reichner, J.S., and Albina, J.E. (2000). Macrophage-Induced Neutrophil Apoptosis. J. Immunol. *165*, 435–441. https://doi.org/10.4049/jimmunol.165.1.435.
13. Guo, S., and DiPietro, L.A. (2010). Factors Affecting Wound Healing. J. Dent. Res. *89*,

219–229. https://doi.org/10.1177/0022034509359125.

14. Khanna, S., Biswas, S., Shang, Y., Collard, E., Azad, A., Kauh, C., Bhasker, V., Gordillo, G.M., Sen, C.K., and Roy, S. (2010). Macrophage Dysfunction Impairs Resolution of Inflammation in the Wounds of Diabetic Mice. PLoS One *5*, e9539. https://doi.org/10.1371/journal.pone.0009539.
15. Koh, T.J., and DiPietro, L.A. (2011). Inflammation and wound healing: the role of the macrophage. Expert Rev. Mol. Med. *13*, e23. https://doi.org/10.1017/S1462399411001943.
16. Haertel, E., Joshi, N., Hiebert, P., Kopf, M., and Werner, S. (2018). Regulatory T cells are required for normal and activin-promoted wound repair in mice. Eur. J. Immunol. *48*, 1001–1013. https://doi.org/10.1002/eji.201747395.
17. Zaidi, M.R., Davis, S., Noonan, F.P., Graff-Cherry, C., Hawley, T.S., Walker, R.L., Feigenbaum, L., Fuchs, E., Lyakh, L., Young, H.A., et al. (2011). Interferon-γ links ultraviolet radiation to melanomagenesis in mice. Nature *469*, 548–553. https://doi.org/10.1038/nature09666.
18. Polisetti, N., Gießl, A., Zenkel, M., Heger, L., Dudziak, D., Naschberger, E., Stich, L., Steinkasserer, A., Kruse, F.E., and Schlötzer-Schrehardt, U. (2021). Melanocytes as emerging key players in niche regulation of limbal epithelial stem cells. Ocul. Surf. *22*, 172–189. https://doi.org/10.1016/j.jtos.2021.08.006.
19. Hong, Y., Song, B., Chen, H.-D., and Gao, X.-H. (2015). Melanocytes and Skin Immunity. J. Investig. Dermatol. Symp. Proc. *17*, 37–39. https://doi.org/10.1038/jidsymp.2015.14.
20. Lévesque, M., Feng, Y., Jones, R., and Martin, P. (2013). Inflammation drives wound hyperpigmentation in zebrafish by recruiting pigment cells to sites of tissue damage. Dis. Model. Mech. *6*, 508–515. https://doi.org/10.1242/dmm.010371.
21. Hirobe, T. (1983). Proliferation of epidermal melanocytes during the healing of skin wounds in newborn mice. J. Exp. Zool. *227*, 423–431. https://doi.org/10.1002/jez.1402270311.
22. Werner, S., Krieg, T., and Smola, H. (2007). Keratinocyte–Fibroblast Interactions in Wound Healing. J. Invest. Dermatol. *127*, 998–1008. https://doi.org/10.1038/sj.jid.5700786.
23. Ketchum, L.D., Cohen, I.K., and Masters, F.W. (1974). Hypertrophic scars and keloids A Collective Review. Plast. Reconstr. Surg. *53*, 140–154. https://doi.org/10.1097/00006534-197402000-00004.
24. Perrot, C.Y., Javelaud, D., and Mauviel, A. (2013). Insights into the Transforming Growth Factor-β Signaling Pathway in Cutaneous Melanoma. Ann. Dermatol. *25*, 135–144. https://doi.org/10.5021/ad.2013.25.2.135.
25. Jeong, H.-W., and Kim, I.-S. (2004). TGF-beta1 enhances betaig-h3-mediated keratinocyte cell migration through the alpha3beta1 integrin and PI3K. J. Cell. Biochem. *92*, 770–780. https://doi.org/10.1002/jcb.20110.
26. Schneider, C.A., Rasband, W.S., and Eliceiri, K.W. (2012). NIH Image to ImageJ: 25 years of image analysis. Nat. Methods *9*, 671–675. https://doi.org/10.1038/nmeth.2089.

STAR★METHODS

KEY RESOURCES TABLE

REAGENT or RESOURCE	SOURCE	IDENTIFIER
Antibodies		
Mouse polyclonal alpha smooth muscle Actin antibody	Thermo Scientific	Cat no. # MS-113-P0; RRID: AB_64001
Rabbit polyclonal Ki67 antibody	Abcam	Cat no.# 15580; RRID: AB_443209
Rabbit monoclonal Vimentin primary antibody	Cell Signaling Technology	Cat no.# 5741; RRID: AB_10695459
Mouse anti Guinea Pig CD4 antibody	Thermo Fisher Scientific	Cat no.# MA1-80842; RRID: AB_928258
Goat anti-Rabbit IgG (H+L) Cross-Adsorbed Secondary Antibody, Alexa Fluor™ 488	Thermo Fisher Scientific	Cat no. # A-11008; RRID: AB_143165
Goat anti-Mouse IgG (H+L) Cross-Adsorbed Secondary Antibody, Alexa Fluor™ 488	Thermo Fisher Scientific	Cat no. # A-32723; RRID: AB_2633275
Goat anti-Rabbit IgG (H+L) Cross-Adsorbed Secondary Antibody, Alexa Fluor™ 568	Thermo Fisher Scientific	Cat no. # A-11011; RRID: AB_143157
Goat anti-Mouse IgG (H+L) Cross-Adsorbed Secondary Antibody, HRP	Thermo Fisher Scientific	Cat no. # G-21040; RRID: AB_2536527
Chemicals, peptides, and recombinant proteins		
Ketamine Hydrochloride	Neon Lab Ltd.	NA
Xylazine	ASRT Agencies	NA
-SYBR® Green based qPCR 2X master mix	G-Biosciences	Cat no.# 786-1980
L-tyrosine	SRL chemicals	Cat no.# 18917
phenylthiourea	SRL chemicals	Cat no.# 16795
Synthetic Melanin	Sigma	Cat No.# M8631
Recombinant human TGF-β	PeproTech	Cat no.# 100-21
Dulbecco's Modified Eagle Medium (DMEM), High glucose	Himedia	Cat No.# AT066
Dulbecco's Modified Eagle Medium/Nutrient Mixture F-12 Ham (DMEM/ F12, 1:1 mixture)	Himedia	Cat No.# AT140
M254 media	Gibco	Cat no.# 24228792
KSFM media	Gibco	Cat no.# 2451167
25 Culture-Inserts 2 Well for self-insertion	ibidi	Cat no.# 80209
Critical commercial assays		
NucleoSpin RNA, Mini kit for RNA purification	Macherey-Nagel	Item no. 740955.50
TGF beta-1 Human ELISA Kit	Thermo Fisher Scientific	Cat no.# BMS249-4
Oligonucleotides		
Table no -	Table S1	
Software and algorithms		
GraphPad Prism		RRID: SCR_002798
ImageJ		RRID: SCR_003070

RESOURCE AVAILABILITY

Lead contact

Further information and requests for resources and reagents should be directed to and will be fulfilled by the lead contact, Archana Singh (archana@igib.res.in).

Materials availability

This study did not generate new unique reagents.

Data and code availability

This paper does not report original code.
Any additional information required to reanalyze the data reported in this paper is available from the lead contact upon request.

EXPERIMENTAL MODEL AND STUDY PARTICIPANT DETAILS

Wound creation in guinea pigs

The study was approved by the Institutional Animal Ethics Committee of National Institute of Immunology, New Delhi & animals were purchased from the animal husbandry department of CCS Haryana agricultural University, India. Disease-free male and female guinea pigs having both pigmented (PG) and non-pigmented (NP) skin with an average age of 3-4 months were included in the study. After anesthetizing the animals with ketamine (doses 100mg/kg weight) and xylazine (doses 10mg/kg weight), full-thickness 1x1 cm^2 wounds were created on the PG as well as NP skin using a sterile scalpel and the wounds cleaned with 10% betadine. Skin removed at day 0 to create the wounds was allowed to heal by secondary intention without any intervention (other than dressing changes) and none of the wounds were found to be infected during the course of the study. Follow-up punch biopsies were taken from the previously wounded sites on the 5^{th}, 9^{th}, 12^{th}, 14^{th}, 17^{th} and 32^{nd} day post wound (n = 5 animals / time point for molecular analysis and n = 3 for histological evaluation) from the centre of the wounds (schematic in Figure S1). Wounds were created on both flanks of each animal that possessed both pigmented (black) and non-pigmented (white) skin. All biopsies were collected after perfusing the animals with 1X PBS containing heparin.

Ethics statement

The study was approved by the Institutional Animal Ethics Committee of National Institute of Immunology, New Delhi.

METHOD DETAILS

Macroscopic evaluation of wounds

Healing of cutaneous wounds was macroscopically assessed from standardized digital photographic images using the Image J software.[26] [7]. The healed area was calculated by subtracting the wounded/non-healed region from the original wound area created. All the wounds closed by day 12 leaving a scar tissue in the centre of the wound. We therefore calculated the scar tissue post-day 12 to access scarring in PG vs. NP skin. The data were statistically analysed for n = 3 animals for each time point.

Histology and special stains

Skin samples were fixed in 4% buffered formalin solution and four-micron thick paraffin-sections collected on glass slides and stained with hematoxylin and eosin for histological evaluation. Staining for melanin (Fontana-Masson) and collagen (Masson's trichrome) was performed on the paraffin sections.

Quantitation of melanin and collagen content

The 64-bit Fontana-Masson stained and Masson trichrome stained images were converted into 8-bit images and melanin was quantified using the threshold method using ImgaeJ tool. For melanin estimation, the ratio of mean gray value to the total area of the ROI (region of interest) for each of the image was calculated. The ratios were plotted with respect to the melanin levels obtained at day 0 (baseline). Collagen content was calculated by selecting the 'Masson Trichrome' module using the deconvolution 2 tool provided in ImageJ, and percentage collagen content was calculated per unit area.

Transmission electron microscopy

Skin samples were fixed in buffered solution containing 2.5% glutaraldehyde and 4% paraformaldehyde and osmicated in 1% osmium tetroxide. Samples were then dehydrated in graded series of ethanol and infiltrated with Epon 812 resin. 62nm thick ultrathin sections were cut on an ultramicrotome (Leica EM UC7), stained with uranyl acetate and lead citrate and imaged on a Tecnai G2 20 twin (FEI) 200KV Transmission Electron Microscope (TEM).

Total RNA extraction, cDNA synthesis and real time PCR

Total RNA was extracted by TRIzol Reagent (Invitrogen) and 1μg of RNA was converted into cDNA (1^{st} strand cDNA synthesis kit, Takara). Real time PCR (RT-PCR) was performed on Roche Light Cycler 480 using SYBR Green chemistry (Fermentas Intl, Ontario, Canada) as per manufacturer's instructions. 18srRNA were used as an internal control.

RT-PCR data analysis

The Ct method (ΔCt value) was used for gene expression analysis. Ct values were normalized to their corresponding 18s rRNA levels to obtain ΔCt values. The reactions were performed in triplicates, and ΔCt values that differed by an SD of 0.5 between the replicates was eliminated from further analysis. For calculating ΔΔCt, the average ΔCt values obtained for the reference day (day0/day5/day9/day14/day32) in non-pigmented skin was subtracted from each of the ΔCt values obtained for the corresponding test day in pigmented skin

(day0/day5/day9/day14/day32). Fold change was calculated using 2^(-ΔΔCt) where ΔΔCt represented ΔCt of pigmented skin on a given day (day0/day5/day9/day14/day32) – ΔCt of corresponding day in non-pigmented skin (day0/day5/day9/day14/day32). RT-PCR results for immune markers were plotted as 'scatter plot with bar' where bar represented average log2FC values ± standard error of mean (SEM), and each point on the bar represented log2FC for each sample.

Primary cultures of normal human epidermal melanocytes (NHEM) and normal human dermal fibroblasts (NHDF)

Human foreskin samples were chopped into smaller pieces, sterilized with 70% ethanol for 1 minute and the samples were incubated at 4°C overnight in 0.25% Dispase-II (Sigma) to aid separation of epidermis from the underlying dermis. Epidermis was incubated in 0.1% trypsin solution for 9 min at 37°C, quenched with trypsin inhibitor (DTI, Gibco) and tissues were seeded in T25 flask in melanocyte-specific M254 media containing growth supplements (Gibco). The dermis was chopped into smaller pieces, digested overnight with 1mg/ml collagenase IV at 37C, and the resulting single cell suspension was cultured in DMEM-HG media containing 10% fetal bovine serum (FBS) to obtain fibroblast cells. All experiments on melanocytes and fibroblasts were performed between passages 2-4.

Modulation of melanin content in melanocytes

Equal number of melanocytes were seeded on day 1 (~$1.25x10^5$ cells/well in 6 well plates) in M254 media. After overnight adhesion, cells were either treated with 100 μM L-tyrosine (added only on day1) or left untreated (basal pigmentation). For some experiments, melanocytes were seeded in double density (~$2.5x10^5$ cells/well in 6 well plates) and treated with 600 μM phenylthiourea (PTU), a melanogenesis inhibitor. Seventy-two hours post treatment with tyrosine or PTU, fresh basal M254 media was added to the melanocytes and incubated for another 24 hours. This media was referred to as 'conditioned media'.

Melanin estimation in melanocytes

Melanocytes were lysed in 250 μl of 1N NaOH solution, incubated at 80C for 2hr on dry bath, centrifuged at 8000rpm for 8 minutes. The absorbance of the resulting supernatant was measured (in duplicates) at 400nm spectrophotometer (Tecan). Synthetic melanin was used to plot the standard curve as per manufacturer's instructions.

Keratinocyte migration assay

The human spontaneous immortal keratinocytes, HaCaT, was procured from ATCC and were cultured in Dulbecco's modified Eagle's medium (DMEM-F12) Ham (AL127A, Himedia) supplemented with 10% fetal bovine serum (FBS) (RM1112, Himedia) containing 1x anti-anti® (penicillin, streptomycin, and amphotericin B , Gibco). Cultures were maintained in a 5% CO_2 humidified atmosphere at 37°C in an incubator (Eppendorf). HaCaT cells were trypsinized and reseeded in 2-chamber slides (C6557, Nunc Labtek II, Thermo) containing culture-inserts (80209, iBidi, Martin Reid, Germany). At around 95-100 percent cell confluence, cells were treated with 7μM/ml Mitomycin C for 2 hours to arrest cell growth. Culture-inserts were removed, fresh media was added along with 25% 'conditioned media' from tyrosine-treated or untreated melanocytes (control cells) and migration of keratinocytes to the wounded area (scratch) was imaged every 4 hours upto 12 hours with a microscope (Floyd). Area remaining between two wound borders was measured by ImageJ and graph was plotted to represent percentage of closed wound (keratinocyte migration) at different time points(hours).

α-SMA and Ki67 staining in fibroblasts

Effect of conditioned media on fibroblast proliferation (Ki67) as well as on its differentiation (alpha-SMA) was evaluated using immunocytochemistry (ICC). Briefly, primary fibroblasts (NHDF) were grown on coverslips, treated with 25% 'conditioned media 'from melanocytes for 24 hours, and fixed with 4% paraformaldehyde. Following permeabilization with 0.01% Triton X-100 and blocking with normal goat serum, cells were either incubated with 1:500 dilution of vimentin (pan-fibroblast marker) and 1:400 dilution of α-SMA antibody, or 1:500 dilution of Ki67 antibody, followed by incubation with 1:1000 Alexafluor 568 and/or Alexafluor 488-conjugated secondary antibody. Hoechst was used for nuclear counterstaining. Imaging was done on a Leica SP8 confocal microscope.

Immunohistochemistry (IHC) of α-SMA and CD4+T cells

For IHC, deparaffinized paraffin-embedded sections were blocked with 5% blocking agent, incubated with primary antibodies specific to human specific α-SMA (1:200 dilution) or guinea pig-specific CD4 (1:100) overnight at 4°C. Sections were incubated with horseradish peroxidase (HRP)-conjugated secondary antibody and visualized them using 3,3-diaminobenzidine (DAB, brown color) to detect the protein of interest. The stained tissue was observed using an inverted optical microscope.

Cell cycle assay

HaCaT keratinocyte cells were trypsinized, fixed in chilled 70% ethanol (in PBS), and incubated for 1 hour with a solution containing 1mg/ml propidium iodide, 0.01% triton-X 100 and RNase A. The DNA content of the cells was then analysed on a flow cytometer (BD Accuri).

ELISA for TGF-β

96 well-plates were coated with the capture antibody (1:250) and further subjected to blocking with 2X blocking buffer (stock 20X; 20X PBS with 1% Tween 20 and 10% BSA) at room temperature for 2 hours. 100 ul of TGFβ standards were used with eight serial dilutions from 10ng/ml to 0.078125 ng/ml. 10 ul of test samples that is conditioned media of the melanocytes (MC CM) and tyrosine-treated melanocytes (MC TYR that is, Melanocytes treated with tyrosine) along with biotin labelled anti-human LAP monoclonal detection antibody (1:250) was incubated for 2 hrs. The wells were incubated with 1:400 dilution of streptavidin-HRP following which ubstrate (Tetramethylbenzidine) was added to each well (15 min, room temperature). The reaction was stopped using 2N H_2SO_4 and absorbance was taken at 450 nm (reference was taken at 570nm) in spectrophotometer (Tecan).

Statistical analysis

Statistical significance was calculated using unpaired, 2-tailed Student's t test, and p values <0.05 were considered statistically significant. All statistical analyses were carried out using Graph-Pad Prism software (version 5, San Diego, USA).